

# Switching Devices Based on Interlocked Molecules<sup>†</sup>

ANTHONY R. PEASE, JAN O. JEPPESEN,  
J. FRASER STODDART,\* YI LUO,  
C. PATRICK COLLIER, AND JAMES R. HEATH

*Department of Chemistry and Biochemistry,  
University of California, Los Angeles, 405 Hilgard Avenue,  
Los Angeles, California 90095-1569*

Received December 12, 2000

## ABSTRACT

An architectural rationale and an experimental program aimed at the development of molecular electronics switching devices for memory and computing applications are discussed. Two-terminal molecular switch tunnel junctions are identified as the critical device components of molecular electronics-based circuitry. They can be tiled in two dimensions and are tolerant of manufacturing defects. Singly and multiply configurable solid-state switching devices that are based upon electrochemically switchable molecular and supramolecular systems are discussed in terms of both the synthesis of the molecular components and the fabrication and performance of the devices.

## Preamble

The area of molecular electronics<sup>1</sup> has advanced considerably during the past few years.<sup>2,3</sup> While there are several reasons for this progress, one enabling factor has been the rapid development in methods for synthesizing<sup>4</sup> not only bistable supramolecular complexes, but also bistable molecular compounds. Now the time is ripe to exploit these advances in both noncovalent<sup>5</sup> and supramolecularly assisted covalent synthesis<sup>6</sup> in the context of solid-state device fabrication. Over the past couple of years, we

Anthony Pease obtained his B.Sc.(Hons) from the University of Salford. He is currently studying toward a Ph.D. in Professor Fraser Stoddart's laboratories at UCLA, where he devotes his time to computational and physical studies of supramolecular processes, while also finding new ways to represent supramolecular phenomena graphically.

Jan O. Jeppesen received his B.Sc. (1996) and M.Sc. (1999) from the University of Odense, where he is currently a Ph.D. student with Professor Jan Becher. He spent 10 months in Professor Fraser Stoddart's group at UCLA working on the template-directed synthesis of switchable rotaxanes.

J. Fraser Stoddart received all his degrees (B.Sc./1964; Ph.D./1966; D.Sc./1980) from the University of Edinburgh. He held academic positions at the Universities of Sheffield (1970–1990) and Birmingham (1990–1997) before moving to the Saul Winstein Chair of Organic Chemistry at UCLA, where he is using the mechanical bond in interlocked molecules to assemble molecular-level machines and devices.

Yi Luo received his Ph.D. in Applied Physics from Columbia University (2000) working in the group of Professor Rich Osgood. He is currently a postdoctoral fellow in the Department of Chemistry at UCLA, working in the area of molecular electronics devices and circuitry.

C. Patrick Collier received his B.A. from Oberlin College (1991) and his Ph.D. in chemistry from UC Berkeley (1998). He is currently a Hewlett-Packard postdoctoral researcher working at the Department of Chemistry at UCLA, working in the area of molecular electronics devices and circuitry.

James R. Heath received his B.Sc. from Baylor University (1984) and his M.A. and Ph.D. from Rice University (1988). He was a postdoctoral fellow at UC Berkeley before joining the research staff at IBM Watson Labs in 1991. In 1994 he moved to UCLA, where he is currently Professor of Chemistry. He works in various areas related to nanoscale science and engineering.

have utilized a number of electrochemically switchable molecular and supramolecular systems as the active elements in solid-state switchable tunnel junction devices. In this Account, the template-directed synthesis<sup>7</sup> and characterization of some bistable, mechanically interlocked, molecular compounds—catenanes and rotaxanes<sup>8</sup>—will be discussed prior to giving an account of the properties of devices that can be fabricated using this unique class of compounds and their supramolecular precursors—the pseudorotaxanes.<sup>9</sup> First, however, we will discuss, compare, and contrast our approach to molecular electronics with other alternatives.

## Introduction

Molecular electronics devices are based on intrinsic molecular properties. Such devices can, in principle, scale down to true molecular dimensions and may also exhibit tremendous thermodynamic efficiencies for information processing,<sup>10,11</sup> especially as compared to silicon-based devices, for example.<sup>12</sup> Molecular dimensions are obviously well beyond the resolution of standard or even state-of-the-art lithographic techniques. This fact means that, in order to fabricate true nanoscale molecular electronics circuits, the molecules themselves represent just one part of the game. Another aspect involves coming up with fabrication methodologies for nanoscale construction that do not rely on lithographic processing. The only obvious alternative to lithographic processing is chemical assembly, and its use in electronic manufacture opens up a third set of issues—namely, what architectures are consistent with both chemical assembly and electronic circuitry? Finally, at some point, it becomes necessary to interface whatever nanoscale architectures are fabricated with the outside world, implying the need for some structure that can interface (or multiplex) large numbers of molecular electronics devices with small numbers of wires. These individual components of molecular electronics circuitry—(i) template-directed (supra)molecular synthesis and device design, (ii) architecture development, (iii) chemical assembly techniques, and (iv) circuit multiplexing—each represent serious and fundamental scientific challenges, to the extent that the collective task appears daunting indeed. However, over the past few years, there has been very rapid progress in many of these areas. In this Account, we will highlight some of those recent advances that have been made by us and our collaborators. As with any other chemical problem, it is important to know what to make, and so we will first rationalize our approach to devices within the context of architectures for molecular electronics. Next, we will discuss the syntheses of some mechanically interlocked compounds, some of which exhibit electrochemically accessible bistability. We will then discuss experiments that reveal how those molecular properties translate into the characteristics of solid-state, two-terminal molecular

<sup>†</sup> Part of the Special Issue on Molecular Machines.

\* To whom correspondence should be addressed. E-mail: stoddart@chem.ucla.edu.

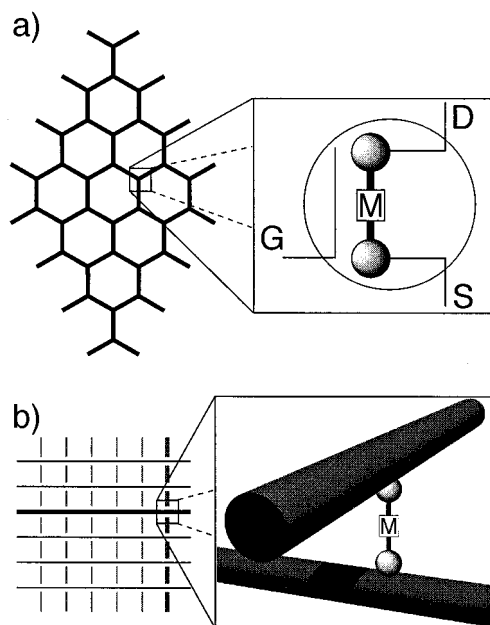


**FIGURE 1.** Two possible device architectures that tile in two dimensions and so may potentially be fabricated through chemical techniques. (a) Three-terminal devices (transistors) arranged in a hexagonal lattice or crossbar structure; (b) two-terminal devices arranged in a square lattice or crossbar structure. Note that there is no way to access an embedded three-terminal device without electrically addressing surrounding devices. However, an appropriate bias on a horizontal wire and a vertical wire can be used to access an embedded two-terminal device. Note that G, S, and D represent the gate, source, and drain terminals of a field effect transistor; M stands for a molecule.

electronics switching devices. Finally, we will look ahead a bit and discuss some of the critical challenges that are likely to be faced soon.

## Architectures and Device Rationale

Any commonly available microprocessor chip is both arbitrarily complex and the product of manufacturing perfection. While both of these traits are critical to the operation of a computer, neither trait can be reproduced by modern chemical synthesis and assembly techniques. In fact, both chemical synthesis (self-assembly) and assembly (self-organization) are characterized by finite yields (implying manufacturing defects), while chemical assembly is typically limited to the production of periodic (crystalline or quasi-ordered) structures. Thus, one aspect of the architecture is that *it must be able to extract perfect complexity from defective order*, and it must do so in a manner that is consistent with standard wiring rules.<sup>13</sup> The architecture that we have used as an initial guide to molecular electronics is based on a computer known as Teramac, which was a massively parallel supercomputer constructed and operated at Hewlett-Packard Laboratories during the past decade.<sup>14</sup> The name Teramac is based on “tera”, for  $10^{12}$  operations per second, and “mac”, for *multiple architecture computer*. Teramac was a chameleon of a computer, meaning that it was not designed as any particular machine, but instead simply contained a tremendous number of resources—i.e., wires and switches—that were laid out according to certain wiring conventions.

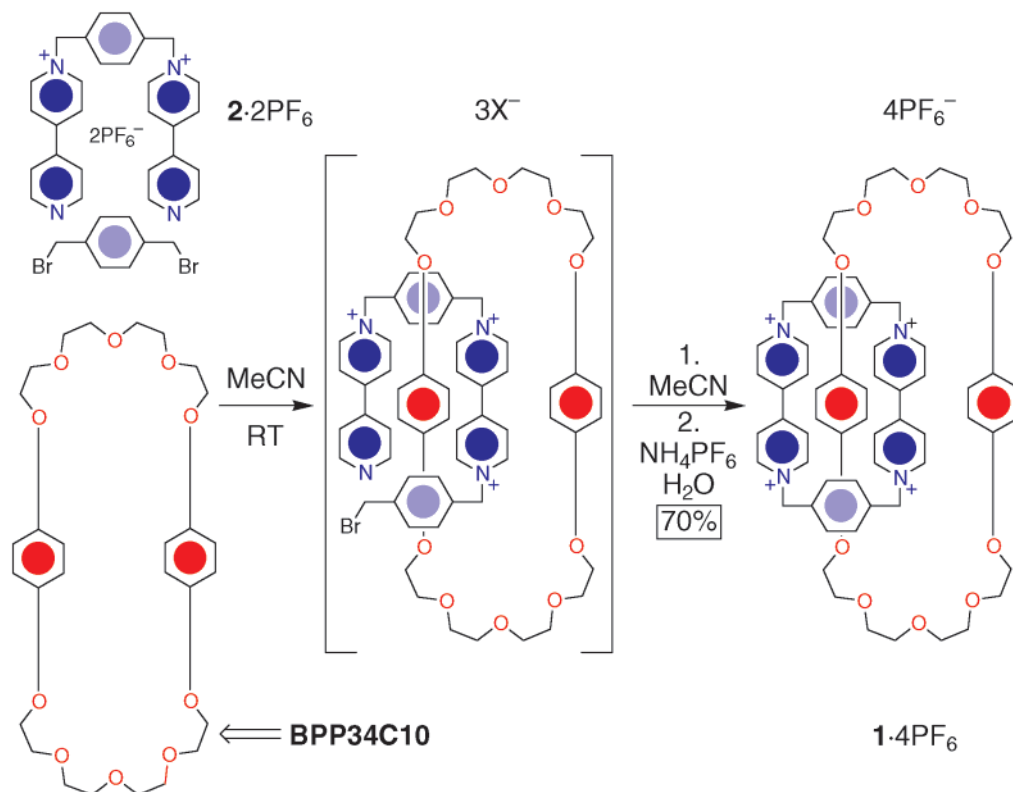


**FIGURE 2.** Template-directed synthesis of the [2]catenane  $1 \cdot 4\text{PF}_6$ . The key step is the spontaneous threading through BPP34C10 of the tricationic intermediate, formed when  $2 \cdot 2\text{PF}_6$  reacts with *p*-xylylene dibromide. This supramolecular assistance is followed by covalent modification and counterion exchange to give  $1 \cdot 4\text{PF}_6$ .

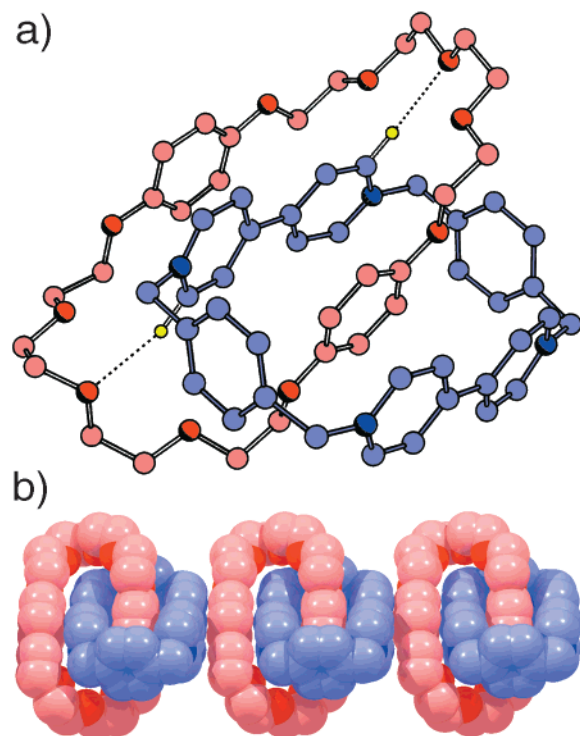


**FIGURE 3.** (a) Ball-and-stick representation of the solid-state structure of  $1^{4+}$ . In addition to the  $[\pi-\pi]$  stacking interactions, the  $[C-H\cdots O]$  hydrogen bonds (dotted lines) represent a significant stabilizing force. (b) Space-filling representation of the polar stack of [2]catenane tetracations in the solid-state superstructure of  $1^{4+}$ .

Teramac could then be configured into any one of a number of customized computing machines by downloading a very long instruction set that effectively mapped the logical structure of the computer onto the hardware resources. In other words, the work required to make a Teramac computer was split between hardware manufacturing and software programming. In fact, one interesting aspect of Teramac is that it allowed researchers to explore the costs and benefits of dividing effort between these two tasks. For example, the hardware manufacturing of Teramac was relatively easy. Teramac was not a perfect machine, but instead contained nearly 250 000 hardware defects, any one of which would kill a modern Pentium machine, for example. However, those defects were paid for in programming effort, as one aspect of the programming was to find configuration routines that could route around defects, as well as to configure logically the intact resources into a computing machine.

At the heart of Teramac were configurable bits, which are properly known as field-programmable gate arrays (FPGAs).<sup>15</sup> While an FPGA is a rather complex device, consisting of four wires into a circuit of six transistors, the FPGAs in Teramac were themselves arranged into a rather simple circuit known as a crossbar (Figure 1). There were many aspects of Teramac that were important for molecular electronics,<sup>16</sup> but among the most critical were the facts that (i) a crossbar of configurable bits is a structure that tiles in two dimensions (2D)—and so is amenable to chemical assembly—and (ii) the crossbar structures, when appropriately configured, were tolerant

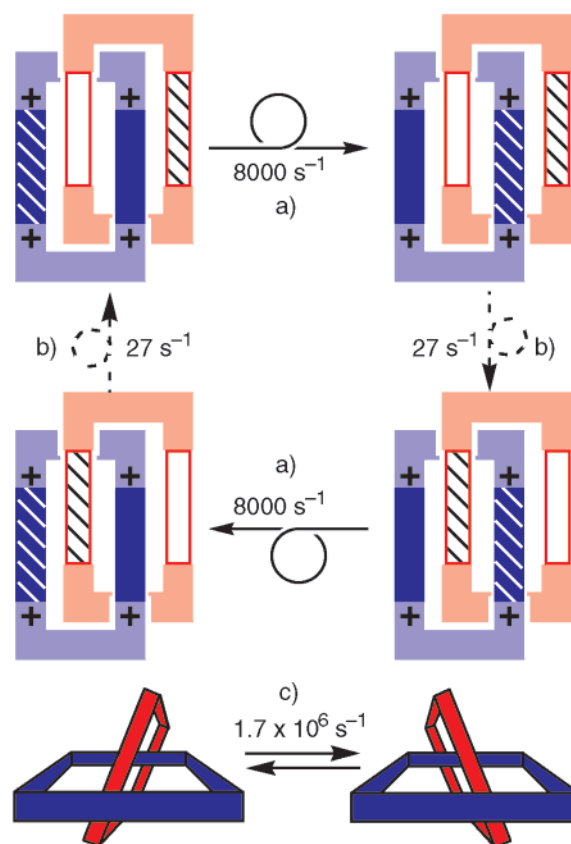


**FIGURE 4.** Three different degenerate co-conformational processes observed in temperature-dependent  $^1\text{H}$  NMR spectra of the [2]-catenane  $1^{4+}$ : (a) circumrotation of  $\text{CBPQT}^{4+}$  through  $\text{BPP34C10}$ ; (b) circumrotation of  $\text{BPP34C10}$  through  $\text{CBPQT}^{4+}$ ; and (c) rocking of  $\text{BPP34C10}$  within  $\text{CBPQT}^{4+}$ . The rates of these processes at room temperature are shown.

of manufacturing defects—implying that finite reaction yields might not be fatal to computation.

The issue of finding a usable circuit that tiles in 2D is critical and implies much about what types of devices are possible. The standard switch of silicon circuitry is the transistor, which is a three-terminal device. It is certainly possible to tile three-terminal devices in 2D (Figure 1a), and three-terminal molecular devices have even been demonstrated recently.<sup>17</sup> However, for the case of a three-terminal device, typically one or more of the wires to the device needs to be independent of every other device, and in a tiled circuit of three-terminal devices, this cannot be the case and so such a circuit is unlikely to be useful. Two-terminal devices can also tile in 2D using a crossbar structure (Figure 1b), and it is possible to gain electrical access to each individual device. For this reason, we have focused our efforts on two-terminal devices, recognizing that there are several implications. First, transistors can be designed to exhibit gain, while two-terminal devices will likely always be dissipative. Second, in a transistor, different tasks (opening, closing, reading) are done with different wires. In a two-terminal device, different tasks have to be achieved with different voltages, and so voltage levels for the various tasks must be extremely well-defined, or a circuit of such devices will only find limited use. In fact, two-terminal-based crosspoint memory architectures

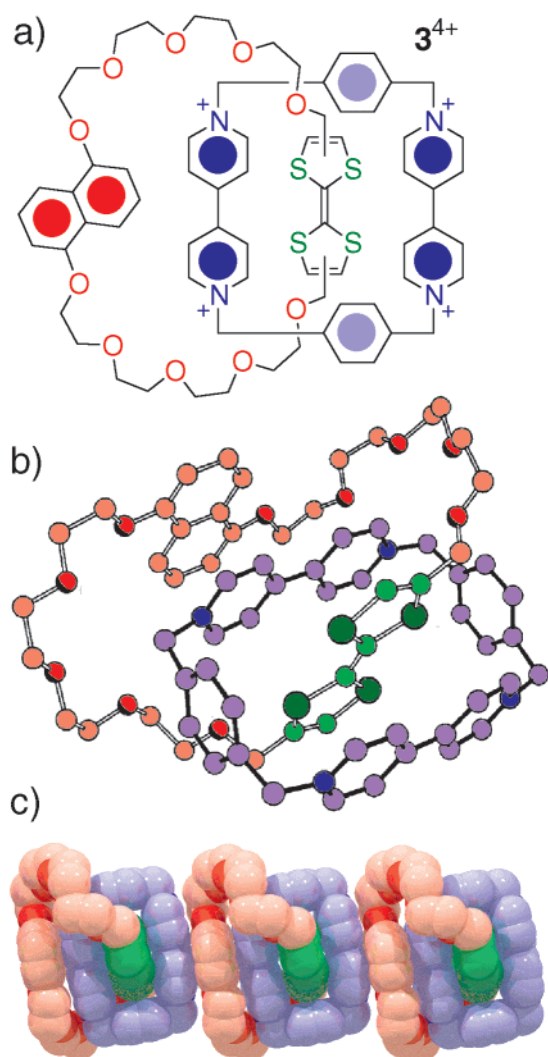


**FIGURE 5.** (a) Structural formula of the [2]catenane  $3^{4+}$ . (b) Ball-and-stick representation of the catenane's solid-state structure showing the TTF unit of the crown ether residing inside the CBPQT $^{4+}$  component. (c) Space-filling representation of its solid-state superstructure. Note the polar  $[\pi-\pi]$  stack.

have been developed that are based on the field-dependent poling of ferroelectric media (Fe-RAM), or on the field-dependent poling of magnetoresistive media (MRAM).<sup>18</sup> However, in both of those cases, the poling process itself is a function of field strength, and so the opening or closing of such junctions is a process that is characterized by nucleation statistics. Consequently, in both Fe-RAM and MRAM crosspoint memories, voltages are not particularly well-defined. This fact has placed severe design and operational constraints on those devices. However, if a molecular device is switched using a redox process, then that is, by nature, a voltage-dependent—rather than a field-dependent—process. In other words, unlike MRAM or Fe-RAM devices, in a redox-switchable molecular-based tunnel junction, current has to flow to switch the molecule, and it can only flow when there is alignment of the energy levels of the electrodes with the redox states of the molecule.

One analogy to the molecular switch that we want is a magnetic bit that is characterized by a hysteretic magnetization versus magnetic field curve. Negative field sets the bit to spin-down, positive field sets the bit to spin-up, and the bit is interrogated at zero-field. For a two-terminal molecular electronics switch, the variables “field” and “magnetization” are replaced by “voltage” ( $V$ ) and “current” ( $I$ ). Thus, different voltages do the different tasks of opening, closing, and reading the device. Most molecular junctions will not exhibit a hysteretic  $I-V$  response, and designing such a response into a molecule is a synthetic challenge. Our approach is to use mechanically interlocked molecules in the form of catenanes or rotaxanes.<sup>8</sup> Such molecules can be designed to exhibit internal mechanical motion wherein one component of the molecule moves with respect to the other component upon oxidation (or reduction) of the molecule. In this case, the voltage required to switch the molecule mechanically is the ionization energy of the molecule plus an activation barrier to ionization. The ionization energy levels can potentially lead to sharp voltages for writing to the device, and the activation barrier lends hysteresis to the device, thereby maintaining its state after it has been written to. One subtle issue here is that we do not want our molecular junctions to hold charge, which would make them capacitors rather than conductors. Instead, the molecules are designed to switch between two charge-neutral conformations—a transformation that, in turn, can have an exponential effect on the tunneling current through the junction.

## Toward Molecular Electronics Devices—Catenanes

Since their first reported<sup>20,21</sup> syntheses in the 1960s, the catenanes—topologically fascinating molecules consisting of two or more interlocked rings—have received an increasing amount of attention<sup>8</sup> during the subsequent three decades. With the advent of supramolecular chemistry<sup>22</sup> during the 1970s, the early low-yielding statistical and demanding covalently templated approaches<sup>21</sup> have given way to much more efficient protocols involving supramolecular assistance to covalent synthesis<sup>6</sup> under both kinetic and thermodynamic control. Among the molecular recognition motifs that have provided the supramolecular assistance, we have witnessed the emergence of metal–ligand interactions,<sup>23,24</sup>  $[C-H\cdots O]$  hydrogen bonds augmented by  $[C-H\cdots\pi]$  and  $[\pi-\pi]$  stacking interactions,<sup>25,26</sup> and hydrogen bonding involving both neutral<sup>27–29</sup> and charged<sup>30,31</sup> systems. In the context of device fabrication, recognition phenomena that are amenable to being altered by changing redox potentials are particularly appealing. Thus, we have directed our attention to redox-active catenanes containing two interlocked rings.

**A Degenerate [2]Catenane.** During the 1980s, two important host–guest recognition systems were established,<sup>4</sup> one after the other—the first was the binding of guests (e.g., paraquat, PQT $^{2+}$ ) containing  $\pi$ -electron-deficient ring systems by macrocyclic polyethers (e.g., bis-*p*-phenylene-34-crown-10, BPP34C10) incorporating  $\pi$ -elec-

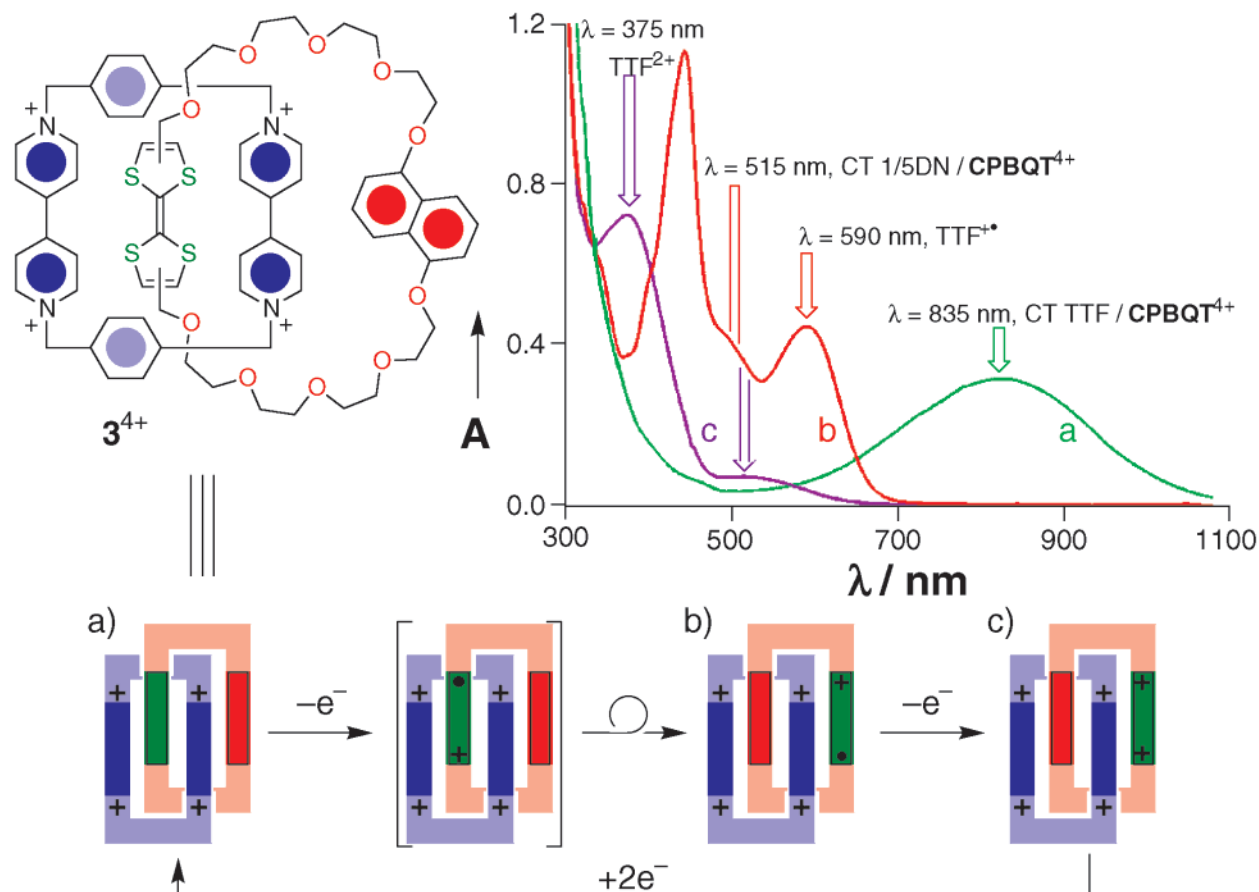


**FIGURE 6.** UV-vis spectroscopic evidence for the redox switching of the [2]catenane  $3^{4+}$  in MeCN ( $9 \times 10^{-5}$  M). (a) Spectrum of the catenane prior to addition of (b) 1 equiv of  $\text{Fe}(\text{ClO}_4)_3$  followed by (c) a second equivalent of  $\text{Fe}(\text{ClO}_4)_3$ . Oxidation is reversed on addition of 2 equiv of ascorbic acid.

tron-rich aromatic rings, and the second was essentially the result of reversing the host-guest roles, leading to the complexation of  $\pi$ -electron-rich guests (e.g., 1,4-dioxybenzene, 1/4DB) by  $\pi$ -electron-deficient hosts (e.g., cyclobis(paraquat-*p*-phenylene),  $\text{CBPQT}^{4+}$ ). The inevitable merger between these two systems led<sup>32</sup> logically to the template-directed synthesis of the [2]catenane  $1^{4+}$ , in which  $\text{CBPQT}^{4+}$  and BPP34C10 are interlocked. It is formed (Figure 2) in a reaction between the dicationic precursor and *p*-xylylene dibromide in the presence of excess of BPP34C10. The catenation is promoted by the noncovalent bonding interactions between the crown ether and a tricationic intermediate which can participate in two significant interactions with BPP34C10—one is  $\pi$ - $\pi$  stacking, and the other is  $[\text{C}-\text{H}\cdots\text{O}]$  hydrogen bonding involving hydrogen atoms  $\alpha$  to the bipyridinium nitrogen atoms and the central oxygen atoms of the polyether loop. In acetonitrile under ambient conditions, the reaction proceeds in the amazingly high yield of 70%—testimony to the strong noncovalent bonding interactions between BPP34C10 and the tricationic precursor to  $\text{CBPQT}^{4+}$ . The manner in which BPP34C10 and  $\text{CBPQT}^{4+}$  interlock with each other can be appreciated from an examination of the solid-state structure (Figure 3a). It reveals a co-conformation in which  $[\pi-\pi]$  stacking and  $[\text{C}-\text{H}\cdots\pi]$  interactions between different aromatic rings are augmented by two strong  $[\text{C}-\text{H}\cdots\text{O}]$  hydrogen bonds. Just

as important in the context of device fabrication is the observation (Figure 3b) that the solid-state superstructure is also highly organized insofar as hydroquinone rings and bipyridinium units are displayed in an infinite donor-acceptor stack that propagates itself along one of the crystallographic directions in a polar manner. Finally, dynamic  $^1\text{H}$  NMR spectroscopy performed on the [2]catenane  $1 \cdot 4\text{PF}_6$  in solution reveals (Figure 4) that, in addition to an extremely rapid rocking motion relating the two interlocked rings, two different degenerate circumrotational processes can be identified. We now have the prototype at three different co-conformational levels—all involving different energy barriers—of a switchable [2]catenane.

**A Redox-Controllable [2]Catenane.** With the passage of time, a [2]catenane  $3^{4+}$  (Figure 5a) containing a tetrathiafulvalene (TTF) and a 1,5-dioxynaphthalene (1/5DN) ring system—each replacing one of the hydroquinone rings in the macrocyclic polyether component of the degenerate [2]catenane  $1^{4+}$ —was obtained<sup>33</sup> in 32% yield employing, as before, a kinetically controlled self-assembly procedure. In designing this potentially switchable [2]catenane  $3^{4+}$ , we had been guided by the fact that, in solution, TTF and its derivative carrying polyether chains display<sup>34</sup> enormously strong binding ( $K_a > 8000 \text{ M}^{-1}$ ) toward  $\text{CBPQT}^{4+}$ , whereas substrates incorporating similarly derivatized 1,5-dioxynaphthalene ring systems<sup>35</sup> are more weakly bound ( $K_a < 5000 \text{ M}^{-1}$ ). While 1/5DN

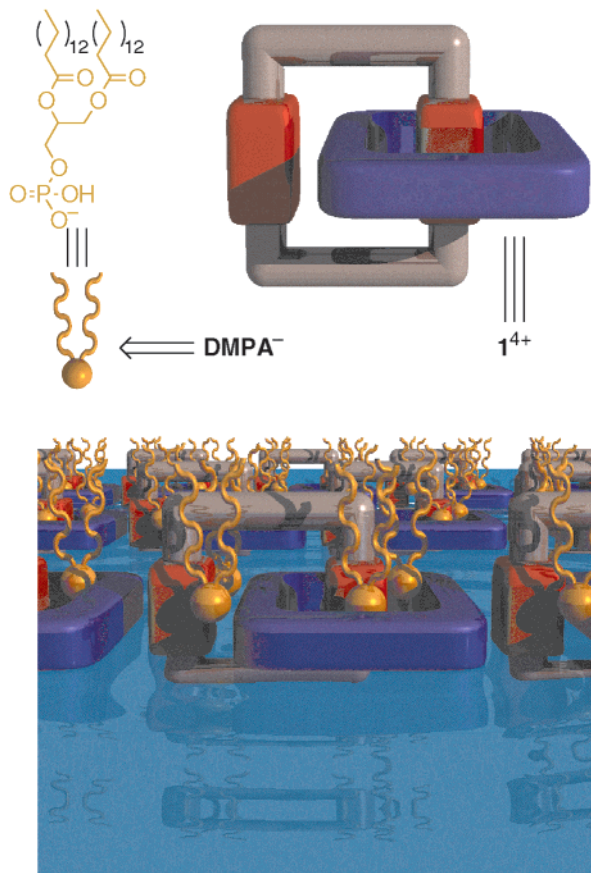


**FIGURE 7.** Schematic representation of the monolayer of  $1\cdot 4\text{DMPA}$  at the air–water interface. Note the intermolecular  $[\pi-\pi]$  stacking interactions between the catenane tetracations.

ring systems are difficult to oxidize, TTF units are readily oxidizable, first to their radical cations ( $E_{1/2} = 320$  mV) and then to their dications ( $E_{1/2} = 720$  mV). Thus, we expected that, although in solutions of  $3^{4+}$  the  $\text{CBPQT}^{4+}$  component would reside preferentially around the TTF unit, upon its oxidation the crown ether component would circumrotate with respect to the  $\text{CBPQT}^{4+}$  component so that the 1/5DN ring system would occupy its cavity. Spectroscopic (UV–vis and NMR) experiments performed<sup>33</sup> on the [2]catenane, both in solution and in the solid state, supported this hypothesis.

X-ray analysis performed<sup>33</sup> on a single crystal of  $3\cdot 4\text{PF}_6$  revealed (Figure 5b) only the translational isomer with the TTF unit residing inside the  $\text{CBPQT}^{4+}$  component and the continuation (Figure 5c) of the molecular donor–acceptor stack beyond the molecule into the supramolecular domain. The solid-state molecular co-conformation is also retained exclusively in solution, as indicated by UV–vis spectroscopy. In the knowledge<sup>33</sup> that acyclic polyether derivatives, incorporating (1) one TTF unit and (2) one 1/5DN ring system, form complexes with  $\text{CBPQT}^{4+}$  with charge transfer (CT) bands centered on 835 and 515 nm, respectively, the UV–vis spectrum (Figure 6) of  $3\cdot 4\text{PF}_6$  can be used to determine the co-conformation and redox state of the [2]catenane. The green acetonitrile solution of  $3\cdot 4\text{PF}_6$  indicates that the TTF unit is encircled by the  $\text{CBPQT}^{4+}$  component. On addition of 2 equiv of the

oxidant  $\text{Fe}(\text{ClO}_4)_3$ , the CT band responsible for the green color at 835 nm disappears completely and is replaced by two bands—one centered on 375 nm for  $\text{TTF}^{2+}$  and another broader band at 515 nm, responsible for the maroon color of this hexacationic species. Addition of 2 equiv of a reducing agent (ascorbic acid) regenerates the green color and restores the UV–vis spectrum to its original form. This redox process, which can be repeated many times, can also be driven electrochemically. A cyclic voltammogram of  $3\cdot 4\text{PF}_6$  reveals<sup>33</sup> that the first oxidation potential of the TTF unit is shifted to a much more positive potential (760 mV) compared with that observed (280 mV) for the crown ether on its own. Likewise, at higher oxidation potentials, we find that the first potential of the 1/5DN ring system has also been shifted by over 400 mV to more oxidizing potentials, indicating the circumrotational motion of the crown ether component in the [2]catenane, following oxidation of the TTF unit.

These results—fascinating as they are—do not, however, constitute the fabrication of a device. Although switching has been demonstrated at the molecular level, it remains little more than a scientific curiosity until coherence can be imposed and some function (e.g., electronic device switching) can be demonstrated.

## Langmuir Monolayers

Recalling the polar stacks of the [2]catenane tetracations present in the solid-state structures of  $1\cdot 4\text{PF}_6$  and  $3\cdot 4\text{PF}_6$  encouraged us to assemble them in two dimensions by forming Langmuir films and then transferring them onto substrates for device evaluation.

**Monolayers of the Degenerate [2]Catenane.** Since the [2]catenane  $1^{4+}$  possesses only polar features, we found it necessary<sup>36</sup> to supply the amphiphilic character in the form of dimyristoylphosphatidyl (DMPA<sup>−</sup>) anions. When cospread—as its  $4\text{PF}_6^-$  salt—onto water with 5 equiv of the sodium salt of DMPA<sup>−</sup>, the  $1^{4+}$  forms very stable monolayers with areas per catenane tetracation of the order of 2.3 nm<sup>2</sup>—an area corresponding to the 10 alkyl chains of the five DMPA<sup>−</sup> anions. It is believed that the monolayer is stabilized (Figure 7) by  $[\pi-\pi]$  stacking interactions between adjacent catenane molecules, aligned such that the cavity of the  $\text{CBPQT}^{4+}$  component is perpendicular to the air–water interface, with the DMPA<sup>−</sup> anions sitting in a tight fully occupied layer above that of the tetracationic catenane. The fact that these monolayers could be transferred to hydrophobized quartz, using the Langmuir–Blodgett (LB) technique, was particularly gratifying with future device construction in mind. In fact, stable multilayers up to 30 bilayers could be obtained with little difficulty—heralding three-dimensional order on top of two-dimensional assembly. For the time being, however, the next question is, does the switchable [2]catenane  $3^{4+}$  also form stable Langmuir films?

**Monolayers with the Switchable [2]Catenane.** Indeed, the redox-active [2]catenane  $3^{4+}$  forms<sup>37</sup> stable monolayers when it is cospread onto an aqueous substrate, this time with 4 equiv of the sodium salt of DMPA. Once again,

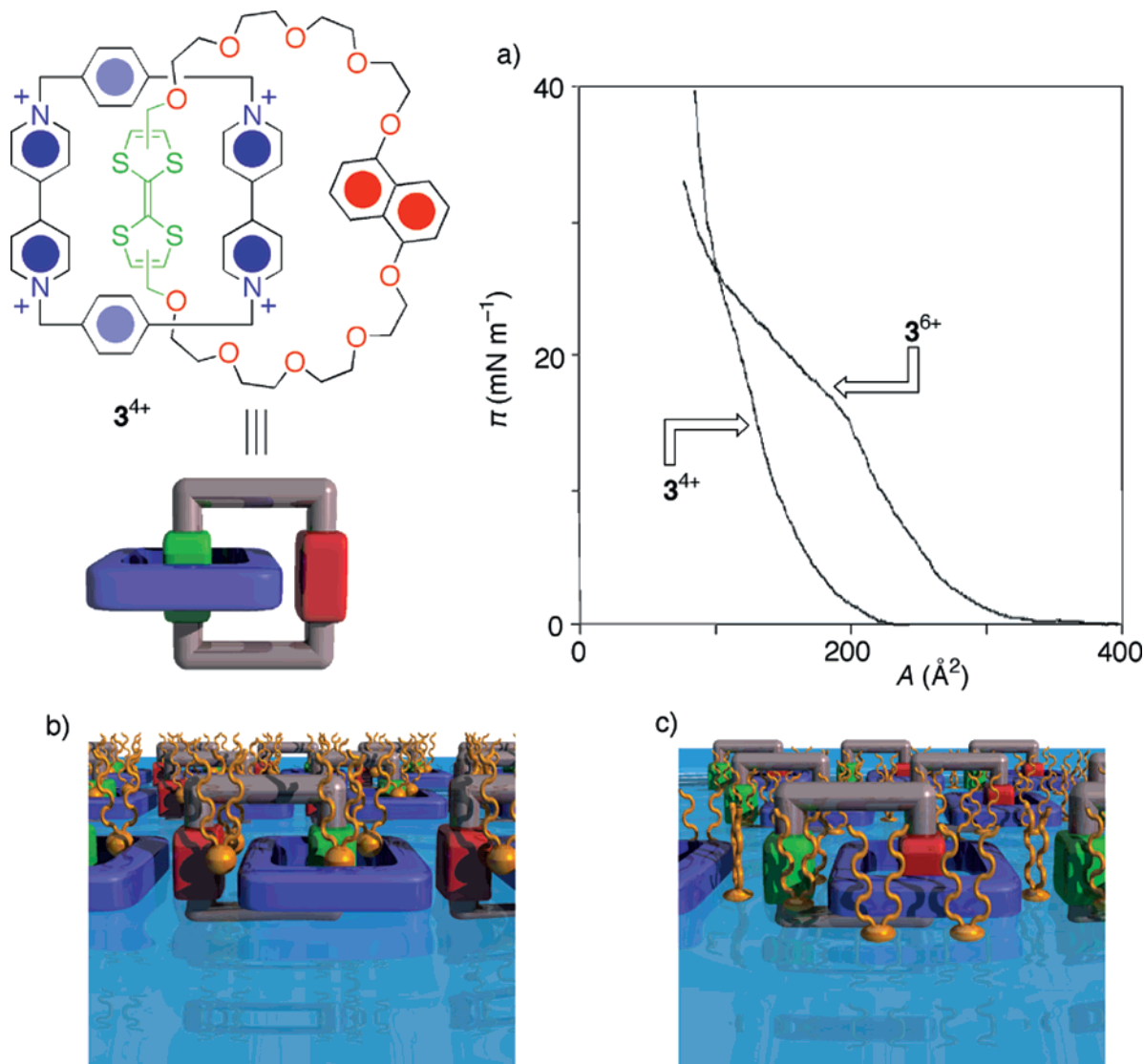


**FIGURE 8.** (a)  $\pi$ - $A$  isotherms of monolayers of the [3]catenane  $3^{4+}$  and its oxidized derivative  $3^{6+}$  anchored with 4 and 6 equiv of DMPA<sup>-</sup> anions, respectively. (b) Schematic representation of the monolayer of  $3^{4+}$ DMPA stabilized by extensive  $[\pi-\pi]$  interactions. (c) Schematic depiction of the first stable monolayer formed by  $3^{6+}$ DMPA. The dicationic TTF units show no affinity for the neighboring catenane hexacations, and so the six DMPA<sup>-</sup> anions fill the voids in the monolayer.

$[\pi-\pi]$  stacking interactions, reminiscent of those observed in the solid-state superstructure (Figure 6c), can be invoked to rationalize at least some of the two-dimensional order. In the case of  $3^{4+}$ , the area per catenane tetracation is found (Figure 8a) to be around 1.2 nm<sup>2</sup> with the four DMPA<sup>-</sup> anions believed to be clustered in a layer above the tetracations (Figure 8b). Upon generation of the hexacation  $3^{6+}$  by treatment of  $3^{4+}$  with 3 equiv of Fe(ClO<sub>4</sub>)<sub>3</sub> and subsequent cospreading with 6 equiv of the Na salt of DMPA, two stable monolayers were observed with areas per catenane of 2.7 and 1.5 nm<sup>2</sup>, respectively. These areas can be interpreted in terms of the anions dictating the area occupied (Figure 8c) when the surface pressure is below 20 mN m<sup>-1</sup>, whereas above 25 mN m<sup>-1</sup> the catenane hexacations start to enter into  $[\pi-\pi]$  stacking interactions and so become determining of the area occupied by the amphiphilic salt. Whatever the nature of the superstructures of the two monolayers, both redox states of the catenane were transferred successfully (below

20 mN m<sup>-1</sup>) by a horizontal lifting technique onto (i) freshly cleaved mica and (ii) the  $\langle 111 \rangle$  face of gold. When the mica-bound monolayers were examined by tapping-mode AFM, it was observed<sup>37</sup> that, while the monolayer containing the catenane  $3^{4+}$  is extremely flat, the catenane  $3^{6+}$  is very bumpy with roughly 25 nm wide and 2 nm high "hills". When the corresponding gold-supported monolayers (Figure 9) were examined by scanning tunneling spectroscopy (STS), important differences were noted between the monolayers containing  $3^{4+}$  and  $3^{6+}$ —the former only conducted current above +0.3 V, whereas the latter exhibited a linear  $I$ - $V$  curve reminiscent of a metal. Given these differences, we felt optimistic about the construction of an electronic device using this switchable catenane.

**A [2]Catenane-Based Electronically Reconfigurable Switch.** LB monolayers of switchable [2]catenane  $3^{4+}$  were incorporated into a sandwich-type device containing *n*-polycrystalline silicon (polySi) bottom electrodes and a

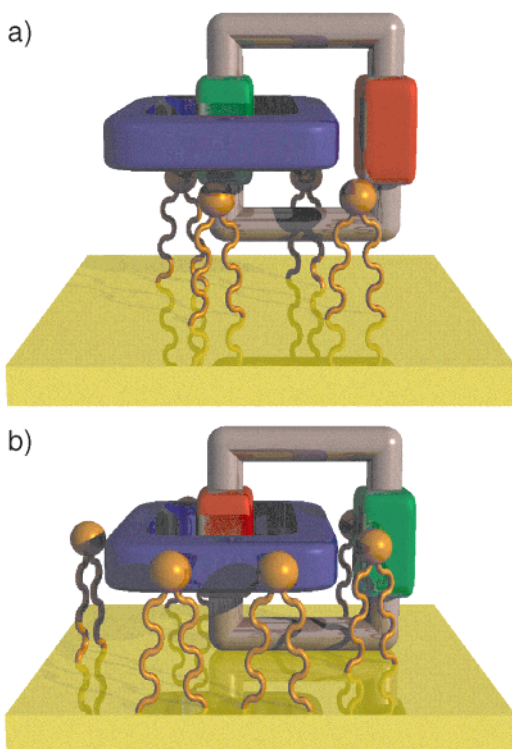


**FIGURE 9.** Nature of the amphiphilic layers when (a) the monolayer containing  $3^{4+}$  is transferred onto a gold substrate (note that the catenane tetracations are insulated from the substrate by DMPA<sup>-</sup> anions) and (b) the monolayer containing  $3^{6+}$  is transferred onto a gold substrate (note the possibility of significant coupling between the substrate and the catenane hexacations).

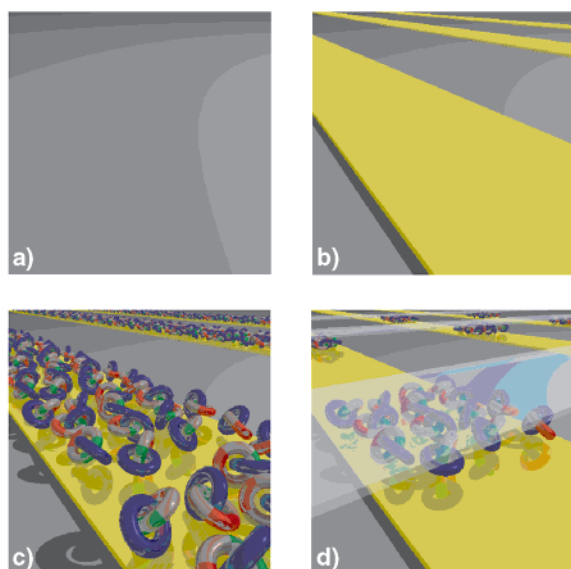


**FIGURE 10.** Construction of a molecular-based device. (a) A smooth silicon substrate. (b) A series of parallel polysilicon wires etched onto the substrate photolithographically. (c) Following deposition of the catenane monolayer onto the wafer by a LB procedure. (d) The result when titanium vapor is condensed through a shadow mask, depositing a second layer of wires aligned perpendicularly with respect to the first.

Ti/Al (15 nm/100 nm) top electrode (Figure 10) in order to evaluate the possibility of fabricating a solid-state switching device. The surface of a grown polySi thin film

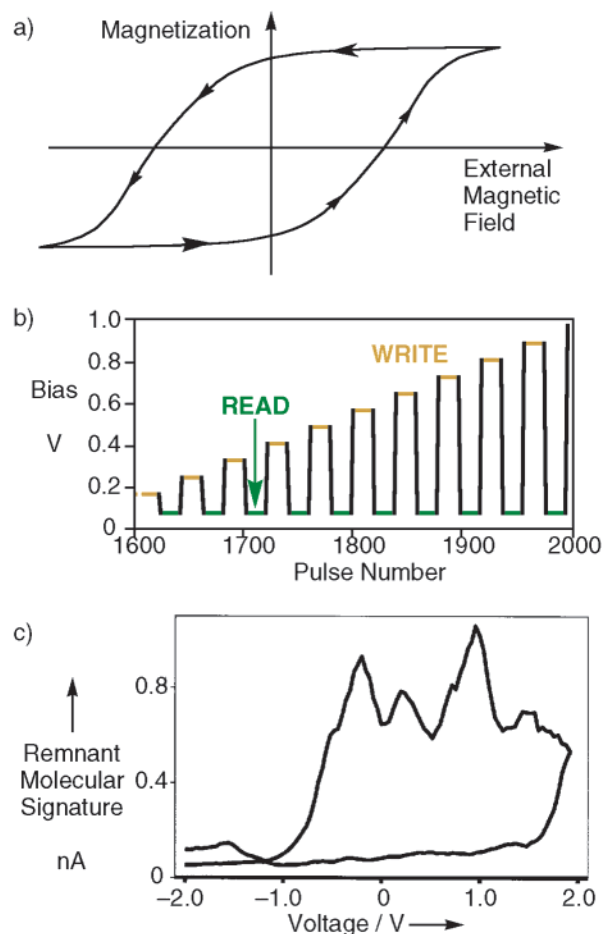


**FIGURE 11.** (a) Hysteresis curve associated with a conventional magnetic memory bit. (b) Voltage profile used in the acquisition of (c) the remnant molecular signature of a device incorporating the switchable [2]catenane  $3^{4+}$ .

is typically too rough to support a clean transfer of a Langmuir monolayer, and so the polySi was formed via a many-step process that involved crystallization of an amorphous silicon thin film. Details of this process have been described elsewhere.<sup>38</sup> The polySi electrodes (5  $\mu\text{m}$  wide) of the device were patterned using standard photolithography techniques. Langmuir monolayers of the bistable [2]catenane were prepared with a 1:6 stoichiometry of  $3 \cdot 4\text{PF}_6 \cdot \text{Na} \cdot \text{DMPA}^-$  on an 18.2 M $\Omega$  water subphase that contained 6.4 mM  $\text{CdCl}_2(\text{aq})$  and was adjusted to pH 8.5 with  $\text{NaOH}(\text{aq})$ . LB films of the bistable [2]catenane were transferred at 1.25 nm<sup>2</sup> per tetracation. Control devices of the degenerate [2]catenane  $1^{4+}$  and  $\text{CBPQT}^{4+}$  were similarly prepared<sup>36,39</sup> and transferred at 1.60 and 0.90 nm<sup>2</sup> per tetracation, respectively. Each film was characterized by a transfer ratio of approximately 1.1. Once the LB films had been transferred, the top electrodes were deposited through a shadow mask, using electron-beam deposition.

To reiterate, it is important that our devices are conductors and not capacitors. Any tunnel junction, such as those described here, will have some residual capacitance. Therefore, in order to measure the switching characteristics of these devices, it is important to do a measurement that is not sensitive to capacitance. Such a



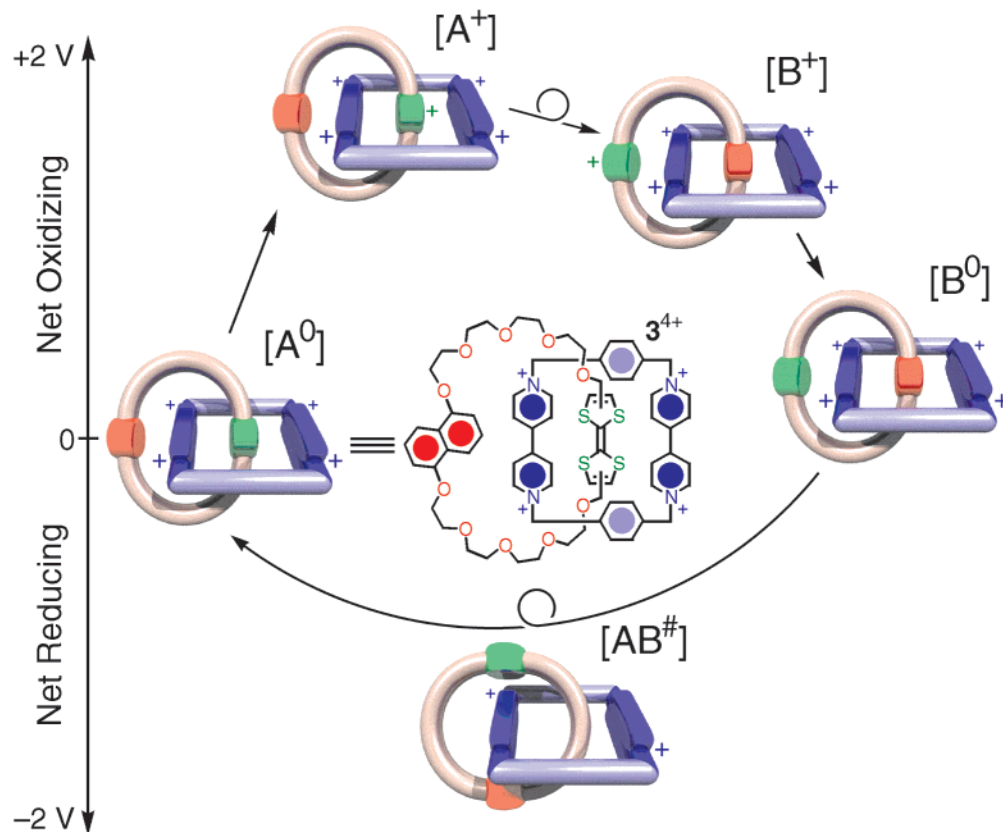


**FIGURE 12.** Proposed mechanochemical mechanism for the operation of the device fabricated from the bistable [2]catenane  $3^{4+}$ . Co-conformation  $[A^0]$  is the “switch open” state and co-conformation  $[B^0]$  the “switch closed” state of the device. When  $3^{4+}$  is oxidized, the TTF unit is ionized in state  $[A^+]$  and experiences a Coulomb repulsion inside the CBPQT $^{4+}$  component, resulting in circumrotation of the crown ether and formation of co-conformation  $[B^+]$ . When the voltage is reduced to near-zero bias, the TTF $^{+}$  unit is reduced to give co-conformation  $[B^0]$ , which does not return to co-conformation  $[A^0]$  by further circumrotation of the crown ether ring via state  $[AB^\#]$  until the cyclophane component is reduced.

measurement in ferroelectric devices (Figure 11a) is known as a remnant polarization curve,<sup>40</sup> and it consists of applying a series of voltage pulses to the device, moving stepwise from the bottom to the top of the hysteresis loop, and then back again. After each voltage pulse, current through the device is read at some low nonperturbing voltage. For our measurements, we charted the hysteresis loop between  $-2.0$  and  $2.0$  V, and we monitored the device response at  $0.1$  V (Figure 11b). We did, in fact, observe robust and significant hysteresis (Figure 11c) in the bistable [2]catenane, but not in the control devices, indicating that the bistable [2]catenane device is, in fact, a solid-state molecular switch. It exhibited a “read” current difference between the open and closed states of approximately a factor of 3, a “close” voltage of about  $1.8$  V, and an “open” voltage of about  $-1.0$  V. The bistable [2]catenane device was fairly stable. It was intermittently cycled many times over a two-month period before it showed signs of failure. Although small differences exist between the solution-phase switching mechanism (Figure 6) and that operating (Figure 12) in the solid-state device, the overall picture is similar.<sup>38,41</sup> The circumrotation of the crown ether is initiated by the oxidation of the TTF unit. However, when the TTF unit is restored to neutrality, the relative positioning of the crown ether and the CBPQT $^{4+}$

components remains the same. It is consistent with our device characteristics—i.e., only when the tetracationic cyclophane is reduced and then reoxidized is the initial state restored. In this manner, bistability is achieved. The results indicate the feasibility of using bistable, mechanically interlocked molecules as solid-state molecular switches.<sup>38</sup>

### Toward Molecular Electronics Devices—Rotaxanes and Pseudorotaxanes

Rotaxanes—a family of interlocked molecules<sup>4,6</sup> where one or more rings encircle a dumbbell-shaped component—have been exploited comprehensively in the construction of solution-state molecular switches. By contrast, in a pseudorotaxane,<sup>9</sup> at least one of the stoppers on the dumbbell-shaped component is absent, with the consequences that the ring(s) can easily slip off or on the rod or the semi-dumbbell-shaped compound; i.e., a pseudorotaxane is a supramolecular species. There are numerous examples of switchable [2]rotaxanes described in the literature.<sup>4</sup> Presently, both [2]rotaxanes and [2]pseudorotaxanes are the subject of intense investigation in our laboratories since preliminary results indicate that they can out-perform switchable [2]catenanes spectacularly in

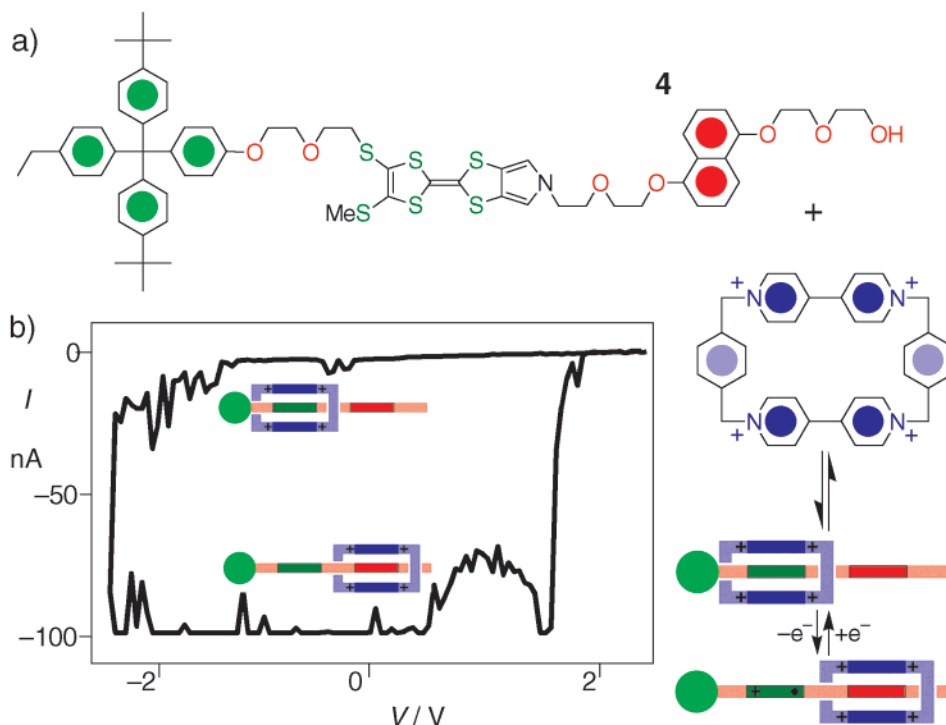


**FIGURE 13.** (a) Bistable pseudorotaxane  $4 \cdot \text{CBPQT}^{4+}$  and (b) the room-temperature solid-state switching signature of this supermolecule. Although the recognition motifs are arranged differently, the bistable character of the pseudorotaxane arises from the same motifs (based on TTF and 1/5DN) as those present in the bistable [2]catenane  $3^{4+}$ . The remnant molecular signature hysteresis loop indicates the possibility of both a large signal amplitude change between the open and closed states and a sharp voltage signature for both closing and opening the device. These two characteristics imply that this switch is superior to the solid-state switch that was fabricated from the [2]catenane.

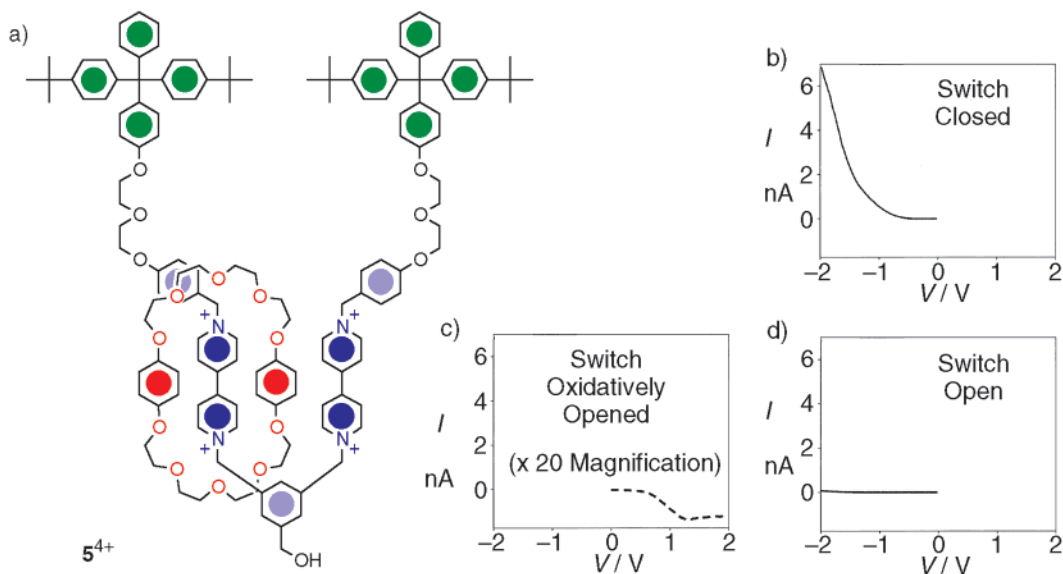


**FIGURE 14.** (a) V-shaped amphiphilic [2]rotaxane  $5^{4+}$ . The current–voltage profile of  $5^{4+}$  when sandwiched between  $\text{Al}/\text{Al}_2\text{O}_3$  and Ti electrodes (b) shows a high current at negative potentials. (c) The switch is cycled once at positive potential, resulting in (d) a permanently opened (fused) switch.

a device setting. The superstructure of a [2]pseudorotaxane  $4 \cdot \text{CBPQT}^{4+}$  that we have successfully demonstrated as a solid-state switch is shown in Figure 13a, and the remnant molecular signature data for a molecular switch tunnel junction fabricated from this supermolecule are shown in Figures 13b. This device, which also used polySi bottom electrodes and a Ti/Al top electrode, was fabricated in a manner nearly identical to that already described for the bistable [2]catenane. These data, which are

presented here for the first time, will not be discussed further, except to highlight an obvious point that is made by Figure 13b—far superior device properties may be designed into these molecular electronics switching devices by optimizing chemical and molecular mechanical properties of the switching (super)molecules.

Certain of the [2]rotaxanes (and indeed [3]rotaxanes) that we have investigated<sup>42</sup> have exhibited bistability that may be accessed only once, although the effect is quite

large. Such bistability is not as ultimately practical as a completely reconfigurable switch. Nevertheless, it has proven extremely useful in that it has allowed us to demonstrate an architectural concept known as “switchable diode logic” that provides a defect-tolerant approach for extracting Boolean logic functions from two-terminal devices.

**Electronically Configurable Molecular-Based Logic Gates.** In a manner similar to that described for the switchable [2]catenane, the V-shaped amphiphilic [2]-rotaxane  $5^{4+}$  (Figure 14a) was sandwiched<sup>42,43</sup> as its  $4PF_6^-$  salt between two electrodes—namely, an Al electrode passivated with the native  $Al_2O_3$  oxide, and a top Ti/Al electrode. As initially deposited, the resonant tunneling of the electrons between the electrodes is facile (Figure 14b), with a relatively large current being passed at voltages below  $-1$  V. This current profile is repeatable and was reproduced multiple times with many devices. However, upon oxidative degradation (Figure 14c) of the [2]-rotaxane  $5^{4+}$ , the resonant tunneling at negative potentials is reduced (Figure 14d) by nearly a factor of 100. This observation has been used<sup>42</sup> to configure AND and OR wired logic gates and to demonstrate the defect-tolerant character of this approach to logic.

## A Moment's Reflection

The field of molecular computing<sup>44</sup> is only in its infancy, and serious challenges lie ahead. However, the field, and even the technology that may arise from this work, hold great promise, and the past couple of years have witnessed several critical advances in the right direction. One thing, however, is certain: only through highly collaborative interdisciplinary research will advances be made. The findings described in Account are the result of research by synthetic and physical chemists, physicists, materials scientists, and electronics engineers. The future of molecular electronics lies in the hands of people with disparate backgrounds.

*We are indebted to Professors Vincenzo Balzani (Bologna) and David Williams (London) for long-standing, highly rewarding collaborations that have helped make the research described in this Account possible. This work was supported by the Defense Advanced Research Projects Agency, the Semiconductor Research Corporation, and the National Science Foundation.*

## References

- Aviram, A.; Ratner, M. A. Molecular Rectifiers. *Chem. Phys. Lett.* **1974**, *29*, 277–283.
- Reed, M. A.; Tour, J. M. Computing with Molecules. *Sci. Am.* **2000**, *282* (6), 86–93.
- Tour, J. M. Molecular Electronics. Synthesis and Testing of Components. *Acc. Chem. Res.* **2000**, *33*, 791–804.
- Philp, D.; Stoddart, J. F. Self-Assembly in Natural and Unnatural Systems. *Angew. Chem., Int. Ed. Engl.* **1996**, *35*, 1154–1196.
- Whitesides, G. M.; Simanek, E. E.; Mathias, J. P.; Seto, C. T.; Chiu, D. N.; Mammen, M.; Gordon, D. M. Noncovalent Synthesis: Using Physical Organic Chemistry to Make Aggregates. *Acc. Chem. Res.* **1995**, *28*, 37–44.
- Fyfe, M. C. T.; Stoddart, J. F. Synthetic Supramolecular Chemistry. *Acc. Chem. Res.* **1997**, *30*, 393–401.
- Templated Organic Synthesis*; Diederich, F., Stang, P. J., Eds.; Wiley-VCH: Weinheim, 2000.
- Molecular Catenanes, Rotaxanes and Knots*; Sauvage, J.-P.; Dietrich-Buchecker, C., Eds.; Wiley-VCH: Weinheim, 1999.
- Ashton, P. R.; Chrystal, E. J. T.; Glink, P. T.; Menzer, S.; Schiavo, C.; Spencer, N.; Stoddart, J. F.; Tasker, P. A.; White, A. J. P.; Williams, D. J. Pseudorotaxanes Formed Between Secondary Dialkylammonium Salts and Crown Ethers. *Chem. Eur. J.* **1996**, *2*, 709–728.
- For an especially good introduction to information science for physical scientists, see: Feynman, R. P. In *Lectures in Computation*; Hey, A. J. G., Allen, R. W., Eds.; Addison-Wesley: Menlo Park, 1966.
- Landauer, R. Irreversibility and Heat Generation in the Computing Process. *IBM J. Res. Develop.* **1961**, *3*, 183–191.
- Packan, P. A. Device Physics: Pushing the Limits. *Science* **1999**, *285*, 2079–2081.
- Here, we are implying something known as Rent's rule, which was discovered by Richard Rent at IBM in the 1960s. Although it was never published by Rent, subsequent work has confirmed its validity. See: Landman, B. S.; Russo, R. L. On Pin Versus Block Relationships for Partitions of Logic Graphs. *IEEE Trans. Comput.* **1971**, *C20*, 1469–1479.
- Kanus, U.; Meissner, M.; Strasser, W.; Pfister, H.; Kaufman, A.; Amerson, R.; Carter, R. J.; Culbertson, B.; Kuekes, P.; Snider, G. Implementations of Cube-4 on the Teramac Custom Computing Machine. *Comput. Graphics* **1997**, *21*, 199–208.
- For an excellent discussion on configurable computing, see: Villasenor, J.; Mangione-Smith, W. Configurable Computing. *Sci. Am.* **1997**, *276* (6), 68–71.
- Heath, J. R.; Kuekes, P. J.; Snider, G.; Williams, R. S. A Defect Tolerant Computing Architecture: Opportunities for Nanotechnology. *Science* **1998**, *280*, 1716–1721.
- Park, H.; Park, J.; Lim, A. K. L.; Anderson, E. H.; Alivisatos, A. P.; McEuen, P. L. Nanomechanical Oscillations in a Single  $C_{60}$  Transistor. *Nature* **2000**, *407*, 57–60.
- Jones, R. E., Jr.; Maniar, P. D.; Moazzami, R.; Zurcher, P.; Witowski, J. Z.; Lii, Y. T.; Chu, P.; Gillespie, S. J. Ferroelectric Non-Volatile Memories for Low-Voltage, Low-Power Applications. *Thin Solid Films* **1995**, *270*, 584–588.
- Parkin, S. S. P.; Roche, K. P.; Samant, M. G.; Rice, P. M.; Beyers, R. B.; Scheuerlein, R. E.; O'Sullivan, E. J.; Brown, S. L.; Bucchigano, J.; Abraham, D. W.; Lu, Y.; Rooks, M.; Trouilloud, P. L.; Wanner, R. A.; Gallacher, W. J. Exchange-Biased Magnetic Tunnel Junctions and Applications to Nonvolatile Magnetic Random Access Memory. *J. Appl. Phys.* **1999**, *85*, 5828–5833.
- Wasserman, E. The Preparation of Interlocked Rings: A Catenane. *J. Am. Chem. Soc.* **1960**, *82*, 4433–4434.
- Schill, G. *Catenanes, Rotaxanes, and Knots*; Academic Press: New York, 1971.
- Lehn, J.-M. *Supramolecular Chemistry*; VCH: Weinheim, 1995.
- Jiménez, M. C.; Dietrich-Buchecker, C.; Sauvage, J.-P. Towards Synthetic Molecular Muscles: Contraction and Stretching of a Linear Rotaxane Dimer. *Angew. Chem., Int. Ed.* **2000**, *39*, 3284–3287.
- Fujita, M. Self-Assembly of [2]Catenanes Containing Metals in Their Backbones. *Acc. Chem. Res.* **1999**, *32*, 53–61.
- Balzani, V.; Credi, A.; Raymo, F. M.; Stoddart, J. F. Artificial Molecular Machines. *Angew. Chem., Int. Ed.* **2000**, *39*, 3348–3391.
- Hamilton, D. G.; Montalti, M.; Prodi, L.; Fontani, M.; Zanello, P.; Sanders, J. K. M. Photophysical and Electrochemical Characterization of the Interactions Between Components in Neutral  $\pi$ -Associated [2]Catenanes. *Chem. Eur. J.* **2000**, *4*, 608–617.
- Hunter, C. A. Synthesis and Structure Elucidation of a New [2]-Catenane. *J. Am. Chem. Soc.* **1992**, *114*, 5303–5311.
- Vögtle, F.; Dunnwald, T.; Schmidt, T. Catenanes and Rotaxanes of the Amide Type. *Acc. Chem. Res.* **1996**, *29*, 451–460.
- Kidd, T. J.; Leigh, D. A.; Wilson, A. J. Organic “Magic Rings”—The Hydrogen Bond-Directed Assembly of Catenanes under Thermodynamic Control. *J. Am. Chem. Soc.* **1999**, *121*, 1599–1600.
- Cantrill, S. J.; Pease, A. R.; Stoddart, J. F. A Molecular Meccano Kit. *J. Chem. Soc., Dalton Trans.* **2000**, 3715–3734.
- Hubin, T. J.; Busch, D. H. Template Routes to Interlocked Molecular Structures and Orderly Molecular Entanglements. *Coord. Chem. Rev.* **2000**, *200–202*, 5–52.
- Anelli, P.-L.; Ashton, P. R.; Ballardini, R.; Balzani, V.; Delgado, M.; Gandolfi, M. T.; Goodnow, T. T.; Kaifer, A. E.; Philp, D.; Pietraszkiewicz, M.; Prodi, L.; Reddington, M. V.; Slawin, A. M. Z.; Spencer, N.; Stoddart, J. F.; Vicent, C.; Williams, D. J. [2]Rotaxanes and

- [2]Catenanes Made to Order. *J. Am. Chem. Soc.* **1992**, *114*, 193–218.
- (33) Balzani, V.; Credi, A.; Mattersteig, G.; Matthews, O. A.; Raymo, F. M.; Stoddart, J. F.; Venturi, M.; White, A. J. P.; Williams, D. J. Switching of Pseudorotaxanes and Catenanes Incorporating a Tetrathiafulvalene Unit by Redox and Chemical Inputs. *J. Org. Chem.* **2000**, *65*, 1924–1936.
- (34) Jeppesen, J. O.; Perkins, J.; Becher, J.; Stoddart, J. F. Slow Shuttling in an Amphiphilic Bistable [2]Rotaxane Incorporating a Tetrathiafulvalene Unit. *Angew. Chem., Int. Ed.* **2001**, *40*, 1216–1221.
- (35) Gillard, R. E.; Raymo, F. M.; Stoddart, J. F. Controlling Self-Assembly. *Chem. Eur. J.* **1997**, *3*, 1933–1940.
- (36) Brown, C. L.; Jonas, U.; Preece, J. A.; Ringsdorf, H.; Seitz, M.; Stoddart, J. F. Introduction of [2]Catenanes into Langmuir Films and Langmuir–Blodgett Multilayers. A Possible Strategy for Molecular Information Storage Materials. *Langmuir* **2000**, *16*, 1924–1930.
- (37) Asakawa, M.; Higuchi, M.; Mattersteig, G.; Nakamura, T.; Pease, A. R.; Raymo, F. M.; Shimizu, T.; Stoddart, J. F. Current/Voltage Characteristics of Redox-Switchable [2]Catenanes on Gold. *Adv. Mater.* **2000**, *12*, 1099–1102.
- (38) Collier, C. P.; Mattersteig, G.; Wong, E. W.; Luo, Y.; Beverly, K.; Sampaio, J.; Raymo, F. M.; Stoddart, J. F.; Heath, J. R. A [2]Catenane-Based Solid State Electronically Reconfigurable Switch. *Science* **2000**, *289*, 1172–1175.
- (39) Ahuja, R. C.; Caruso, P.-L.; Möbius, D.; Wildburg, G.; Ringsdorf, H.; Philp, D.; Preece, J. A.; Stoddart, J. F. Molecular Organization via Ionic Interactions at Interfaces. Monolayers and LB Films of Cyclic Bisbipyridinium Tetracations and Dimyristoylphosphatidic Acid. *Langmuir* **1993**, *9*, 1534–1544.
- (40) Lines, M. E.; Glass, A. M. *Properties and Applications of Ferroelectric and Related Materials*; Clarendon Press: Oxford, 1977; p 103.
- (41) Gase, T.; Grando, D.; Chollet, P.-A.; Kajzar, F.; Murphy, A.; Leigh, D. A. Linear and Unanticipated Second-Order Nonlinear Optical Properties of Benzylic Amide [2]Catenane Thin Films: Evidence of Partial Rotation of the Interlocked Molecular Rings in the Solid State. *Adv. Mater.* **1999**, *11*, 1303–1306.
- (42) Collier, C. P.; Wong, E. W.; Belohradsky, M.; Raymo, F. M.; Stoddart, J. F.; Keukes, P. J.; Williams, R. S.; Heath, J. R. Electronically Configurable Molecular-Based Logic Gates. *Science* **1999**, *285*, 391–394.
- (43) Wong, E. W.; Collier, C. P.; Belohradsky, M.; Raymo, F. M.; Stoddart, J. F.; Heath, J. R. Fabrication and Transport Properties of Single-Molecule-Thick Electrochemical Junctions. *J. Am. Chem. Soc.* **2000**, *122*, 5831–5840.
- (44) Pease, A. R.; Stoddart, J. F. Computing at the Molecular Level. *Struct. Bonding* **2001**, *99*, 189–236.

AR000178Q